Article

Kinetic Modeling of Ethanol Batch Fermentation by *Escherichia Coli* FBWHR Using Hot-Water Sugar Maple Wood Extract Hydrolyzate as Substrate

Yang Wang and Shijie Liu *

Department of Paper and Bioprocess Engineering, State University of New York-College of Environmental Science and Forestry, Syracuse, NY 13210, USA; E-Mail: ywang52@syr.edu

* Author to whom correspondence should be addressed; E-Mail: sliu@esf.edu;
Tel.: +1-315-470-6885; Fax: +1-315-470-6501.

Abstract: A recombinant strain of *Escherichia coli* FBWHR was used for ethanol fermentation from hot-water sugar maple wood extract hydrolyzate in batch experiments. Kinetic studies of cell growth, sugar utilization and ethanol production were investigated at different initial total sugar concentrations of wood extract hydrolyzate. The highest ethanol concentration of 24.05 g/L was obtained using an initial total sugar concentration of 70.30 g/L. Unstructured models were developed to describe cell growth, sugar utilization and ethanol production and validated by comparing the predictions of model and experimental data. The results from this study could be expected to provide insights into the process performance, optimize the process and aid in the design of processes for large-scale production of ethanol fermentation from woody biomass.

Keywords: kinetic modeling; hemicellulose; hydrolyzate; xylose; *Escherichia coli*; ethanol; batch fermentation

1. Introduction

With depleting fossil energy sources, increased oil prices and environmental awareness, more public attention has been drawn to the development of alternate forms of chemicals, materials, and energy [1,2].

Ethanol is attractive due to the widespread use as alternative liquid fuel and other fine chemicals such as acetaldehyde and 1,3-butadiene [3], and has been mostly produced by fermentation from feedstocks such as corn and sugarcane [4]. However, debates exist as corn prices have increased significantly with the appearance of competition with food and animal feed [5,6]. Therefore, low-cost lignocellulosic materials such as woody biomass, agricultural residues, processing by-products and energy crops have been considered promising sources for fuel ethanol. Woody biomass is the most abundant organic source on Earth, with annual production in the biosphere of about 5.64×10^{10} Mg-C [7–9]. Hemicellulose containing both hexoses (glucose, galactose, mannose, rhamnose) and pentoses (xylose and arabinose), compromises up to 40% of the carbohydrates content of woody biomass and currently represents the largest polysaccharide fraction wasted in most cellulosic ethanol pilot and demonstration plants around the world [10] and even in corn ethanol plants [6], which would be the largest potential supply to provide ethanol in a world thirsty for liquid transportation fuel.

In the last two or three decades, several microorganisms, such as *Escherichia coli*, *Klebsiella oxytoca*, *Zymomonas mobilis* and *Saccharomyces cerevisiae*, have been developed with a goal of fermenting both hexoses and pentoses to ethanol. *E. coli* is advantageous in ethanol production not only due to its ability to ferment many different types of sugars, but also no requirements for complex growth factors. The major disadvantages of *E. coli* are a narrow and neutral pH growth range, less hardy cultures compared to yeast, biotoxicity and negative public perception regarding the danger of *E. coli* strains [11]. *E. coli* FBR5 has been developed to improve performance and is reported to produce high yields of ethanol [12–16]. Ethanol production from different hydrolyzates by recombinant strain *E. coli* FBR5 has also been investigated [17,18]. Recently, Liu *et al.* [19] have reported ethanol fermentation by *E. coli* FBR5 and its robust mutant FBHW using hot-water sugar maple wood extract hydrolyzate. After being repeatedly challenged and adapted by hot-water sugar maple wood extract hydrolyzate, a new improved strain, *E. coli* FBWHR, which had a good performance and can resist in high concentration of wood hydrolyzate was obtained [20]. In this paper, *E. coli* FBWHR was selected to perform a kinetic modeling study of ethanol batch fermentation.

Establishment of a fermentation kinetic model is important in describing microorganism behavior and metabolic regulation [21]. With technical, economic and physiological implications, it would be a powerful instrument to predict and control problem fermentations, and helpful to understand the fermentation process [22]. Many mathematical models of fermentation processes have been developed as an indispensable step on account of their ability to provide useful information for the analysis of experimental data, reactor design and optimization of operation conditions for the production of a target bioproduct [23–26]. Both structured and unstructured models have been developed for kinetic modeling. Compared to unstructured kinetic models, structured models can explain complex microbial systems at the molecular level, but relatively simpler unstructured kinetic models such as the Monod model and Luedeking–Piret (LP) model [27,28] have been used more widely for practical applications,. Qureshi *et al.* [13] have investigated some parameters of ethanol fermentation by *E. coli* FBR5 such as tolerance to increase level of xylose and ethanol, effect of buffer and inhibitory sodium chloride. Kinetic parameters such as Michaelis-Menten constant, specific growth rate constant, maximum specific growth rate constant and the specific rate of ethanol production were also evaluated. To our knowledge, there are no literature reports on the kinetic performance and kinetic modeling of ethanol fermentation by *E. coli* FBR5 and its mutant strains in complex hot-water sugar maple wood

extract hydrolyzate. Therefore, the objective of this study is focused on kinetic modeling of batch fermentations at different concentrations of hot-water sugar maple wood extract hydrolyzate, including a logistic model for cell growth and models for sugar consumptions and product synthesis.

2. Results and Discussion

As investigated previously, the hot-water sugar maple hemicellulosic wood extracts hydrolyzate used in this study contained six monosaccharides, primarily xylose, and minor amounts of glucose, mannose, arabinose, galactose, and rhamnose and other compounds, such as phenolics and aromatics [7]. Liu *et al.* [19] have reported that the mutant *E. coli* FBHW could grow in concentrated hot-water wood extract hydrolyzate. After successive adaptation of *E. coli* FBHW, a mutant was isolated and named as *E. coli* FBWHR, which was used in this kinetic and modelling fermentation studies. The initial cell concentrations were constant at 0.080 ± 0.005 g/L in this series of batch experiments.

2.1. Kinetics of Batch Ethanol Fermentation of Various Concentrations of Concentrated Hot-Water Sugar Maple Wood Extract Hydrolyzate by E. Coli FBWHR

Figure 1 presents the patterns of utilization of total and individual sugars, biomass growth and ethanol production by recombinant *E. coli* FBWHR with various initial concentrations of concentrated hot-water wood extract hydrolyzate.
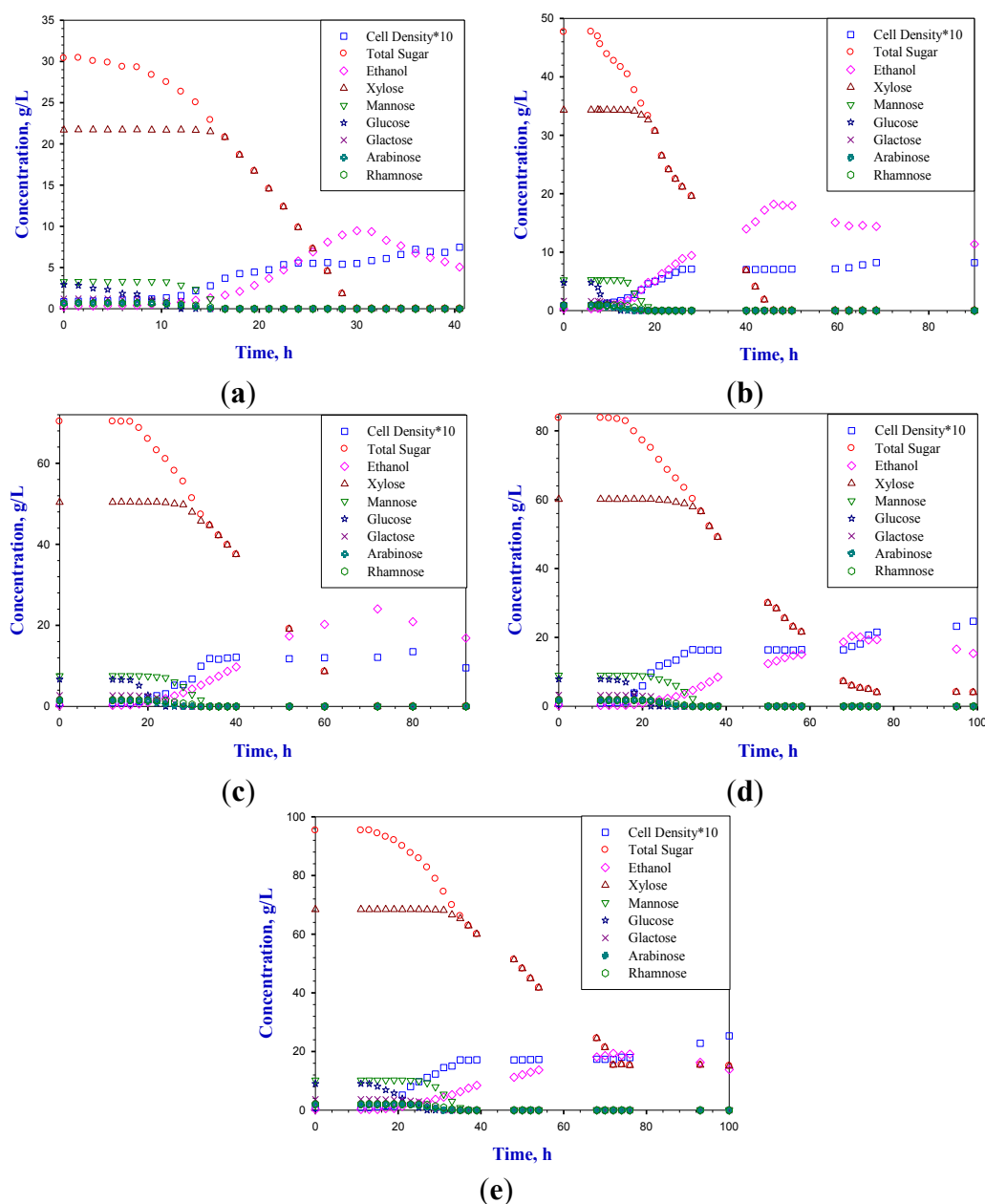
The fermentation with an initial total sugar concentration of 30.39 g/L in 20% (v/v) concentrated hot-water wood extract hydrolyzate was detailed in [20]. For the first 6 h, only 1.04 g/L of total sugar was utilized, and 0.021 g/L of biomass and 0.169 g/L of ethanol were produced. The subsequent exponential growth shows a biomass concentration increase from 0.107 g/L to 0.535 g/L between 6 h and 22.5 h. The diauxic lag phase lasted 7.5 h. Sugars were completely consumed within 30 h of batch fermentation. The ethanol concentration decreased significantly in the last 8 h of fermentation, possibly due to its evaporation and consumption to aid cell growth [5].

As shown in Figure 1a, glucose was utilized first and completely consumed by 12 h into the fermentation, which indicated that recombinant *E. coli* FBWHR preferred to consume glucose than other monosaccharides. Meanwhile, other monosaccharides started to be utilized slowly. Galactose and arabinose were used up in 15 h. However, the consumption rate of galactose was much faster than that of arabinose. Rhamnose and mannose were utilized completely by 16.5 h. However, xylose has not decreased at all by 13.5 h, and was consumed slowly when other monosaccharides were still in the fermentation media. After 16.5 h of batch fermentation, the consumption rate of xylose started to increase, since it was the only monosaccharide left. Xylose was depleted within 30 h.

As shown in Figure 1b, a lag phase was observed in the first 6 h immediately after inoculation in the growth medium by 30% (v/v) concentrated hot-water wood extract hydrolyzate with the initial total sugar concentration of 47.66 g/L. The lag phase is a period of adaptation of *E. coli* FBWHR to the new concentrated hot-water wood extract hydrolyzate environment. Glucose was utilized first and completely consumed by 12.5 h, followed by galactose and arabinose. However, rhamnose was completely utilized earlier than mannose. After 20 h of batch fermentation, xylose was dominantly utilized by *E. coli* FBWHR without the competition of other monosaccharides. The biomass increased exponentially from 6 h to 26 h and reached to 0.705 g/L at 26 h. *E. coli* FBWHR utilized 26.57 g/L

total sugars and produced 8.59 g/L ethanol. The diauxic lag phase was about 20 h. A final ethanol concentration of 18.19 g/L was achieved.

Figure 1. Time courses of recombinant *E. coli* FBWHR growth, total and individual sugar utilization and ethanol production: (**a**) using 20% (v/v) concentrated hot-water wood extract hydrolyzate; (**b**) using 30% (v/v) concentrated hot-water wood extract hydrolyzate; (**c**) using 40% (v/v) concentrated hot-water wood extract hydrolyzate; (**d**) using 50% (v/v) concentrated hot-water wood extract hydrolyzate; and (**e**) using 60% (v/v) concentrated hot-water wood extract hydrolyzate.

(**a**)

(**b**)

(**c**)

(**d**)

(**e**)

As increasing the proportion of concentrated hot-water wood extract hydrolyzate to 40% (v/v) (the initial total sugar concentration to 70.30 g/L), the lag phase extended to 12 h (Figure 1c), because of higher total sugar and inhibitor concentrations. The order of sugar utilization follows a sequence of glucose, galactose, arabinose, mannose, rhamnose and xylose. Glucose was consumed first,

right after which were galactose and arabinose. Mannose started to be utilized by *E. coli* FBWHR after most of the glucose was consumed, then followed by rhamnose. Since the concentration of mannose was much higher than that of other sugars except xylose in the wood extract hydrolyzate, it was used up only before xylose, although its consumption started earlier. Xylose was the last sugar to be utilized by *E. coli* FBWHR. The pattern of sugar utilizations (glucose > arabinose > xylose) in this study confirmed with earlier findings [12,29].

As shown in Figure 1c, the biomass concentration increased exponentially from 16 h to 34 h, and reached to 1.182 g/L at 34 h. *E. coli* FBWHR utilized 25.63 g/L total sugars and produced 6.05 g/L ethanol. A diauxic lag phase was shown by using 40% (v/v) of concentrated hot-water wood extract hydrolyzate, which was about 36 h. The concentration of total sugar was declined by 44.67 g/L and the ethanol yield increased by 17.65 g/L. In 72 h, the total sugar concentration was depleted. The similar phenomenon was found that the ethanol concentration decreased after reaching the maximum by cell growth.

Sugar utilization, biomass growth and ethanol production by recombinant *E. coli* FBWHR at 50% (v/v) concentrated hot-water wood extract hydrolyzate are depicted in Figure 1d. A total sugar concentration of 83.75 g/L was detected. The concentration level of *E. coli* FBWHR was maintained the same in the first 10 h. Then, the exponential phase of cell growth was observed between 10 h and 32 h and the biomass concentration reached 1.645 g/L. During this period, the total sugar concentration was reduced by 20.32 g/L and 4.38 g/L of ethanol was produced. At 50% (v/v) of concentrated hot-water wood extract hydrolyzate, the diauxic lag phase lasted 38 h, which was from 32 h to 70 h. The ethanol production of 20.38 g/L was obtained. *E. coli* FBWHR continued growing after the diauxic lag phase and reached to the highest biomass concentration of 2.469 g/L at 99 h. The ethanol production level did not increase further by continuing the fermentation up to 99 h. However, the concentration of ethanol decreased. There was about 3.99 g/L of residual total sugar remained in the fermentation broth media.

Figure 1e depicts the sugar consumption, biomass growth and ethanol production by recombinant *E. coli* FBWHR at 60% (v/v) of concentrated hot-water wood extract hydrolyzate with a total sugar concentration of 95.33 g/L. The lag phase of ethanol fermentation lasted about 13 h. The biomass concentration increased exponentially between 13 h and 35 h and reached 1.713 g/L with a total sugar consumption of 29.17 g/L. Ethanol production was 6.05 g/L. The diauxic lag phase lasted 37 h, which was between 35 h and 72 h. The ethanol concentration of 13.08 g/L was produced with the consumption of 50.82 g/L total sugar. The maximum ethanol concentration of 19.34 g/L was achieved. In the fermentation media, a xylose concentration of 15.35 g/L remained unutilized.

2.2. Comparison of Different Concentrations of Concentrated Hot-Water Wood Extract Hydrolyzate in Batch Fermentation of E. Coli FBWHR

In this study, lag phase did not occur for ethanol fermentation with 20% (v/v) concentrated hot-water wood extract hydrolyzate, but for increased concentrations of concentrated hot-water wood extract hydrolyzates. Duration of lag time may vary when the medium is switched from xylose and Lysogeny broth (LB) to concentrated hot-water wood extract hydrolyzates due to the change of the physiochemical environment [30]. Another important possible cause is that the period for adaptation of

E. coli FBWHR to a more challenging environment may be prolonged, as the concentration of inhibitors increased by the increases of volume percentage of concentrated hot-water wood extract hydrolyzates.

It also can be observed that no residual sugar concentration was detected when 40% (v/v) or lower concentrated hot-water wood extract hydrolyzate was used. However, a significant level of unutilized sugar was found as further increasing the proportion of concentrated hot-water wood extract hydrolyzate in the fermentation media. This impact was mainly due to the inhibition caused by increasing the concentration of concentrated hot-water wood extract hydrolyzate. Moreover, a similar pattern of sugar utilization was found with the different initial total sugar concentrations of concentrated hot-water wood extract hydrolyzate by *E. coli* FBWHR as described previously.

It can be observed that the biomass concentration reaching the diauxic lag phase increased with the increase of the initial sugar concentration, which means a higher concentration of initial sugar do favor the biomass growth. The biomass concentrations increased sharply by elevating concentrated hot-water wood extract hydrolyzate from 20% (v/v) to 50% (v/v). However, the inhibitor concentration played an important role for cell growth, especially in high concentrated hot-water wood extract hydrolyzate. The biomass concentration rose only about 0.1 g/L, when the concentration of concentrated hot-water wood extract hydrolyzate was increased from 50% (v/v) to 60% (v/v).

Ethanol concentration started to increase with the increase of biomass during the fermentation process. However, more ethanol was produced when the diauxic lag phase was reached. The specific ethanol production rate during the diauxic lag phase was much faster than that during the exponential growth phase. Based on the data, ethanol production does not necessarily follow cell growth. A shorter diauxic lag phase was demonstrated at 20% (v/v) concentrated hot-water wood extract hydrolyzate, because sugars were completely utilized in 30 h. In contrast, a longer diauxic lag phase was presented when using more concentrated hot-water wood extract hydrolyzate. The final ethanol concentration of 18.19 g/L was achieved with 30% (v/v) concentrated hot-water wood extract hydrolyzate, which was about twice higher than that of 20% (v/v) concentrated hot-water wood extract hydrolyzate. The highest ethanol concentration of 24.05 g/L was achieved in this series of kinetic study by using 40% (v/v) concentrated hot-water wood extract hydrolyzate. However, further increasing the concentration of concentrated hot-water wood extract hydrolyzate did not benefit the ethanol production due to the effect of high inhibition from acids, phenolic and aromatic compounds. Although the diauxic lag phase at 50% (v/v) and 60% (v/v) concentrated hot-water wood extract hydrolyzate was 38 h and 37 h, the ethanol concentrations were only 20.38 g/L and 19.34 g/L, respectively. The inhibitors played an important role of the reduction of ethanol production, because although the concentrations of sugars increased when the proportion of concentrated hot-water wood extract hydrolyzate in the fermentation media was increased, in the meanwhile the inhibitor concentrations also increased proportionally.

2.3. Kinetic Model of Different Concentrations of Concentrated Hot-Water Wood Extract Hydrolyzate in Batch Fermentation of E. Coli FBWHR

2.3.1. Cell Growth

The logistic equation is a very common unstructured model in macroscopic description of cell growth processes [31–33]. It is a substrate-independent model, describing a basic law of population
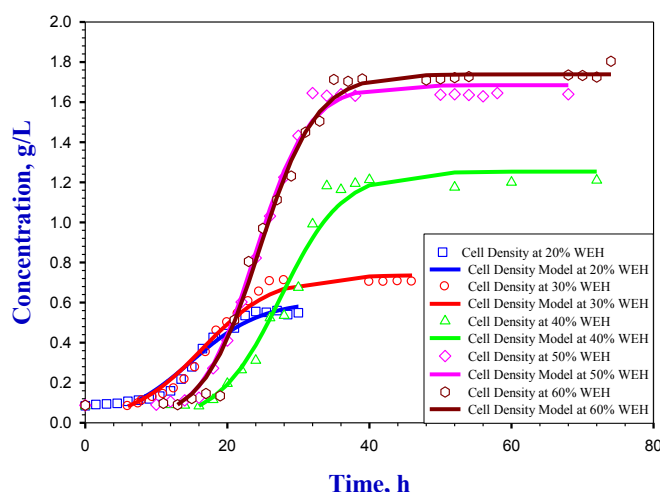
growth in a limited space. Therefore, the logistic equation was adapted to investigate *E. coli* FBWHR growth this study. The logistic equation can be written as follows:

$$\frac{dX}{dt} = \mu_{max} X \left(1 - \frac{X}{X_{max}}\right)$$ (1)

where X is the cell biomass (dry weight) concentration (g/L) at time t; t is fermentation time (h); μ_{max} is the maximum specific growth rate (h^{-1}); and X_{max} is the maximum cell biomass (dry weight) concentration (g/L).

Biomass concentrations at different concentrations of concentrated hot-water wood extract hydrolyzate are fitted to the above logistic equation and are illustrated in Figure 2.

Figure 2. Experimental data and model results of recombinant *E. coli* FBWHR growth during concentrated hot-water wood extract hydrolyzate fermentation.

The values of μ_{max} and X_{max} are listed in Table 1.

Table 1. Kinetic parameters of recombinant *E. coli* FBWHR growth during fermentation at different concentrations of concentrated hot-water wood extract hydrolyzate.

Kinetic parameters	20% (v/v)	30% (v/v)	40% (v/v)	50% (v/v)	60% (v/v)
μ_{max} (h^{-1})			0.229 ± 0.030		
X_{max} (g/L)	0.607	0.737	1.254	1.684	1.739
R^2	0.988	0.991	0.987	0.997	0.995

It can be observed that the model fits well with the experimental results in Figure 2. The high R^2 values of the model (which are higher than 0.985) also presented that the model was able to accurately describe the experimental data of cell growth. It can be noticed that the results of X_{max} increased as the concentrations of concentrated wood extract hydrolyzate increased. The cell biomass concentrations increased significantly by increasing the wood extract hydrolyzate concentration from 20% (v/v) to 50% (v/v). However, further increase of concentrated wood extract hydrolyzate concentration to 60% (v/v), the cell biomass concentration only increased 0.065 g/L compared to the X_{max} of 50% (v/v) wood extract hydrolyzate. The experimental data of X_{max} were comparable to the simulated values. The maximum specific growth rate of 0.229 ± 0.030 h^{-1} was obtained by the logistic equation.

2.3.2. Substrate Utilization and Production Synthesis

Six monosaccharides, primarily xylose and minor amounts of glucose, mannose, arabinose, galactose, and rhamnose, were detected in hot-water sugar maple hemicellulosic wood extracts hydrolyzate [7]. Based on the monosaccharide consumptions patterns of the batch fermentation kinetic studies, assumptions were established in order to estimate parameters of monosaccharides utilizations accurately. Because the periods of galactose and arabinose consumption were very close, in some cases at the same time, it was assumed that galactose and arabinose were consumed at the same time. The same assumption was made for mannose and rhamnose. According to the sequence of monosaccharide utilization and the stoichiometry of monosaccharide utilization, the equations were written as follows:

$$-\frac{dS_{Glu}}{dt} = \frac{\alpha_{Glu}}{YF_{X/Glu}}\frac{dX}{dt} + \frac{\alpha_{Glu}}{YF_{P/Glu}}\frac{\gamma_{p,Glu} \times S_{Glu}}{K_{s,Glu} + S_{Glu}} \tag{2}$$

$$-\frac{dS_{Gal}}{dt} = \frac{(1-\alpha_{Glu}) \times \alpha_{GA}}{YF_{X/GA}}\frac{dX}{dt} + \frac{(1-\alpha_{Glu}) \times \alpha_{GA}}{YF_{P/GA}}\frac{\mu_{GA} \times S_{Gal}}{K_{s,GA} + S_{Gal} + \frac{180.16}{150.13}S_{Ara}} \tag{3}$$

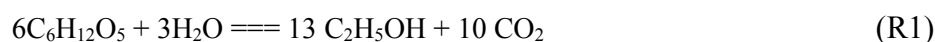$$-\frac{dS_{Ara}}{dt} = \frac{(1-\alpha_{Glu}) \times \alpha_{GA}}{YF_{X/GA}}\frac{dX}{dt} + \frac{(1-\alpha_{Glu}) \times \alpha_{GA}}{YF_{P/GA}}\frac{\mu_{GA} \times S_{Ara}}{K_{s,GA} + S_{Gal} + \frac{180.16}{150.13}S_{Ara}} \tag{4}$$

The molecular weights of hexoses and pentoses are 180.16 g/mol and 150.13 g/mol, respectively. Therefore, $\frac{180.16}{150.13}$ is the conversion factor between pentoses and hexoses. Since the maximum theoretical yields of pentoses and hexoses are 0.51 g ethanol/g sugar, $\gamma_{p,Gal} = \gamma_{p,Ara} = \mu_{GA}$:

$$-\frac{dS_{Rha}}{dt} = \frac{(1-\alpha_{Glu}) \times (1-\alpha_{GA}) \times \alpha_{RM}}{1.189\,YF_{X/Man}}\frac{dX}{dt}$$

$$+ \frac{(1-\alpha_{Glu}) \times (1-\alpha_{GA}) \times \alpha_{RM}}{YF_{P/RM}}\frac{\frac{0.608}{0.51}\mu_M \times S_{Rha}}{K_{s,RM} + \frac{180.16}{164.15}S_{Rha} + S_{Man}} \tag{5}$$

$$-\frac{dS_{Man}}{dt} = \frac{(1-\alpha_{Glu}) \times (1-\alpha_{GA}) \times \alpha_{RM}}{YF_{X/Man}}\frac{dX}{dt}$$

$$+ \frac{(1-\alpha_{Glu}) \times (1-\alpha_{GA}) \times \alpha_{RM}}{YF_{P/RM}}\frac{\mu_M \times S_{Man}}{K_{s,RM} + \frac{180.16}{164.15}S_{Rha} + S_{Man}} \tag{6}$$

The molecular weight of rhamnose is 164.15 g/mol. Therefore, $\frac{180.16}{164.15}$ is the conversion factor between rhamnose and hexoses. Since the maximum theoretical yields of rhamnose and hexoses are 0.608 ethanol/g rhamnose and 0.51 g ethanol/g sugar, respectively:

$$6C_6H_{12}O_5 + 3H_2O === 13\,C_2H_5OH + 10\,CO_2 \tag{R1}$$

$$YF_{P/Rha} = \frac{13 \times 46.068}{6 \times 164.15} = 0.608 \tag{7}$$

Therefore:

$$\mu_M = \gamma_{p,Man} = \frac{0.51}{0.608}\gamma_{p,Rha} \tag{8}$$

According to the available electrons numbers of mannose and rhamnose, the correlation of yield factor between mannose and rhamnose was shown as follows:

$$C_6H_{12}O_6: (4 \times 6 + 12 - 2 \times 6)/6 = 4; \quad C_6H_{12}O_5: (4 \times 6 + 12 - 2 \times 5)/6 = 13/3 \tag{9}$$

$$YF_{X/Rha} = \frac{(13/3)/164.15}{4/180.16} = 1.189 \, YF_{X/Man} \tag{10}$$

$$-\frac{dS_{Xyl}}{dt} = \frac{(1 - \alpha_{Glu}) \times (1 - \alpha_{GA}) \times (1 - \alpha_{RM}) \times \alpha_{Xyl}}{YF_{X/Xyl}} \frac{dX}{dt}$$
$$+ \frac{(1 - \alpha_{Glu}) \times (1 - \alpha_{GA}) \times (1 - \alpha_{RM}) \times \alpha_{Xyl}}{YF_{P/Xyl}} \frac{\gamma_{p,Xyl} \times S_{Xyl}}{K_{s,Xyl} + S_{Xyl}} \tag{11}$$

where $-dS/dt$ is the rate of substrate utilization; S_S is the substrate concentration (g/L), s: Glu, Gal, Ara, Rha, Man, Xyl stand glucose, galactose, arabinose, rhamnose, mannose and xylose, respectively; $\gamma_{p,s}$ is the ethanol production rate from a carbon substrate; $YF_{X/S}$ is the yield coefficient for biomass on carbon substrate (g cells/g substrate); $YF_{P/S}$ is the yield coefficient for product on carbon substrate (g product/g substrate); $K_{S,s}$ is the half saturation coefficient; a, b, c and d are the constants.

In the above model, we have modeled the fractional contribution of different substrates to the rates as follows:

$$\alpha_{Glu} = \frac{S_{Glu}}{a + S_{Glu}} \tag{12}$$

$$\alpha_{GA} = \frac{S_{Gal} + \frac{180.16}{150.13} S_{Ara}}{b + S_{Gal} + \frac{180.16}{150.13} S_{Ara}} \tag{13}$$

$$\alpha_{RM} = \frac{\frac{180.16}{164.15} S_{Rha} + S_{Man}}{c + \frac{180.16}{164.15} S_{Rha} + S_{Man}} \tag{14}$$

$$\alpha_{Xyl} = \frac{S_{Xyl}}{d + S_{Xyl}} \tag{15}$$

and:

$$\alpha_{Glu} + \alpha_{GA} + \alpha_{RM} + \alpha_{Xyl} = 1 \tag{16}$$

where α_S is the fractional rate contribution of substrate S.

As shown from the kinetic data, it was observed that ethanol production occurred during both exponential phase and stationary phase. Therefore, the differential equation of ethanol production is described below:

$$\frac{dP}{dt} = \alpha_{Glu} \times \frac{\gamma_{p,Glu} \times S_{Glu}}{K_{s,Glu} + S_{Glu}} + (1 - \alpha_{Glu}) \times \alpha_{GA} \times \frac{\mu_{GA} \times (S_{Gal} + S_{Ara})}{K_{s,GA} + S_{Gal} + \frac{180.16}{150.13} S_{Ara}} + (1 - \alpha_{Glu})$$
$$\times (1 - \alpha_{GA}) \times \alpha_{RM} \times \frac{\mu_M \times (\frac{0.608}{0.51} S_{Rha} + S_{Man})}{K_{s,RM} + \frac{180.16}{164.15} S_{Rha} + S_{Man}} + \left(1 - \frac{S_{Glu}}{a + S_{Glu}}\right) \times (1 - \alpha_{GA}) \tag{17}$$
$$\times (1 - \alpha_{RM}) \times \alpha_{Xyl} \times \frac{\gamma_{p,Xyl} \times S_{Xyl}}{K_{s,Xyl} + S_{Xyl}}$$

where dP/dt is the rate of ethanol production.

The experimental data and model results for monosaccharide consumption are shown in Figure 3. As seen in the figure, the model accurately described the experimental data of monosaccharides consumptions based on the R^2 values, which were higher than 0.98 in this sugars utilization study. A comparison of ethanol production profiles and model predictions are presented in Figure 4. High values of R^2 ($\geq$0.99) were obtained, which meant that the model predictions could explain equal or more than 99% of total variations for the ethanol production results.

Figure 3. Experimental data and model results of monosaccharides utilizations by recombinant *E. coli* FBWHR during concentrated hot-water wood extract hydrolyzate fermentation: (**a**,**b**) using 20% (v/v) concentrated hot-water wood extract hydrolyzate; (**c**,**d**) using 30% (v/v) concentrated hot-water wood extract hydrolyzate; (**e**,**f**) using 40% (v/v) concentrated hot-water wood extract hydrolyzate; (**g**,**h**) using 50% (v/v) concentrated hot-water wood extract hydrolyzate; and (**i**,**j**) using 60% (v/v) concentrated hot-water wood extract hydrolyzate.
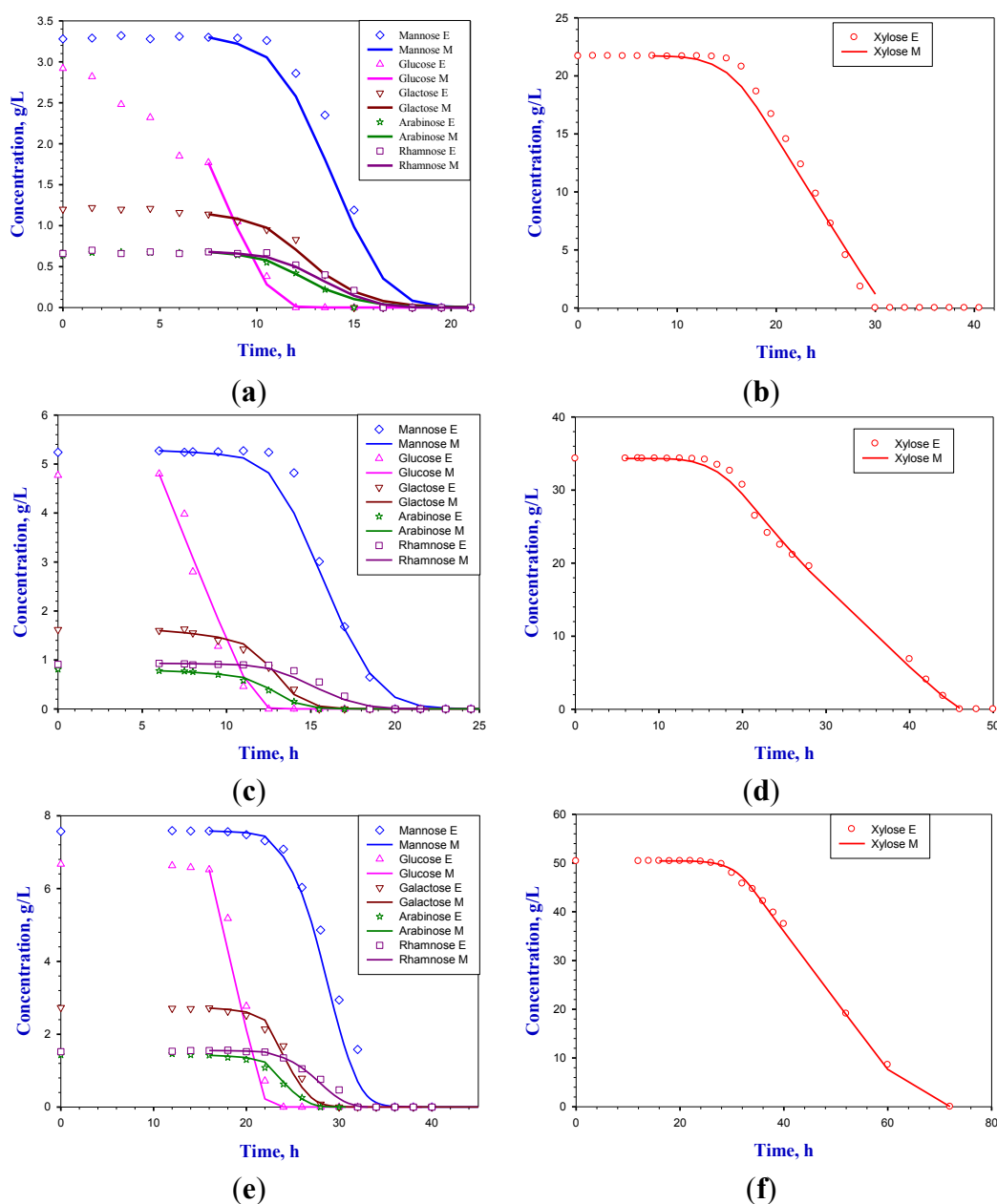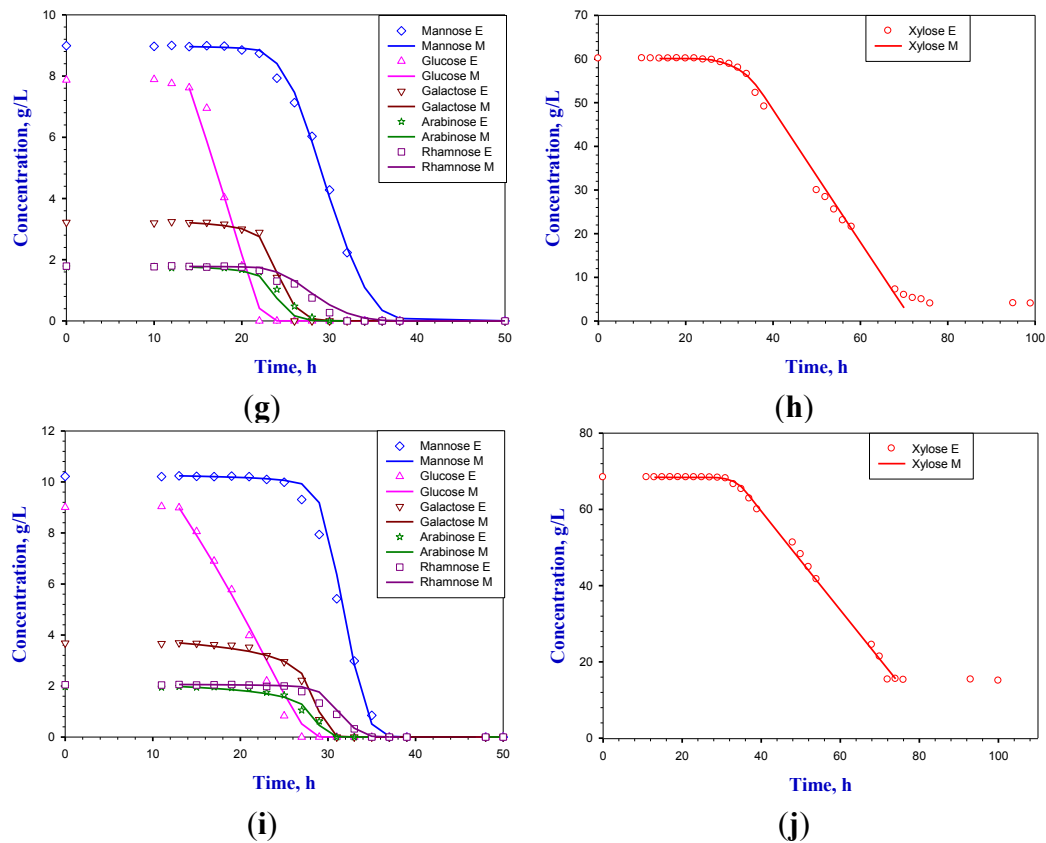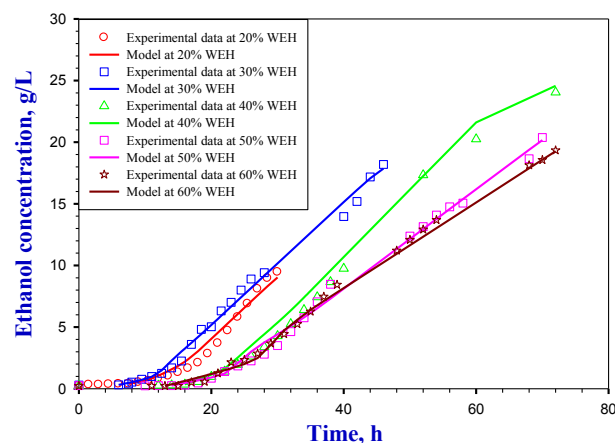
Figure 3. *Cont.*

(g)

(h)

(i)

(j)

Figure 4. Experimental data and model results of ethanol production by recombinant *E. coli* FBWHR during fermentation from concentrated hot-water wood extract hydrolyzate.

The optimal model parameters estimated for different concentrations of concentrated hot-water wood extract hydrolyzate in batch fermentation of *E. coli* FBWHR are presented in Table 2. It can be observed that the yield coefficients for biomass on carbon substrates were low, mainly because the air flow rate was only 0.031 vvm for the ethanol batch fermentation by *E. coli* FBWHR which was considered to be under microaerobic conditions. Cell growth was limited under this condition by the availability of dissolved oxygen in the fermentation broth. The yield coefficients for biomass on carbon substrates decreased with an increase of concentrations of concentrated hot-water wood extract hydrolyzate, which indicated that a smaller proportion of carbon substrates were utilized for

cell growth. Glucose was the monosaccharide that was consumed first. However, the ethanol production rates and the yield coefficients for ethanol on glucose were low, because energy spilling and cell maintenance could occur in this stage. Galactose and arabinose was utilized by *E. coli* FBWHR, which was followed by glucose. The ethanol production rates and the yield coefficients for ethanol on galactose and arabinose were much higher than those on glucose. One possible reason was that as fermentation proceeded, more cells were available to convert sugars to ethanol. However, the ethanol production rates and the yield coefficients for ethanol on mannose and rhamnose were lower than those on galactose and arabinose, which implied that galactose and arabinose were easier to be used by *E. coli* FBWHR than mannose and rhamnose. Xylose was the last sugar to be utilized by the *E. coli* strain. By the time xylose was consumed, cell growth reached the diauxic lag phase. The major task for *E. coli* FBWHR at diauxic lag phase was to utilize xylose to produce ethanol. The ethanol production rate by xylose reached to the maximum for each concentration of concentrated hot-water wood extract hydrolyzate. Compared to 50% (v/v) and 60% (v/v) of concentrated hot-water wood extract hydrolyzate, ethanol production rates were higher with lower percentages of concentrated hot-water wood extract hydrolyzate. Overall, the highest ethanol production rate was 0.550 g/(g·h) by 40% of concentrated hot-water wood extract hydrolyzate. The maximum yield coefficients for ethanol on xylose was 0.486 g ethanol/g xylose by 40% (v/v) of concentrated hot-water wood extract hydrolyzate, which implied that xylose was the most efficient to be converted to ethanol by *E. coli* FBWHR. Based on the results of the half saturation coefficiency, the stage of xylose conversion to ethanol was the rate control for each concentration of concentrated hot-water wood extract hydrolyzate, because the values of $K_{S,Xyl}$ were the highest.

Table 2. Model parameters of ethanol production by fermentation with recombinant *E. coli* FBWHR using different concentrations of concentrated hot-water wood extract hydrolyzate.

Model parameters	20% (v/v)	30% (v/v)	40% (v/v)	50% (v/v)	60% (v/v)
$YF_{X/Glu}$ (g/g)	0.074	0.072	0.063	0.058	0.050
$\gamma_{P,Glu}$ (g/(g·h))	0.081	0.088	0.184	0.090	0.115
$K_{S,Glu}$ (g/L)			1×10^{-12}		
$YF_{P/Glu}$ (g/g)	0.137	0.100	0.165	0.111	0.231
a			0.210 ± 0.000		
$YF_{X/GA}$ (g/g)	0.074	0.072	0.063	0.058	0.050
μ_{GA} (g/(g·h))	0.345	0.68	0.521	0.603	0.989
$K_{S,GA}$ (g/L)			1×10^{-12}		
$YF_{P/GA}$ (g/g)	0.51	0.51	0.51	0.51	0.415
b			1.05 ± 0.003		
$YF_{X/Man}$ (g/g)	0.074	0.072	0.063	0.058	0.050
μ_M (g/(g·h))	0.110	0.436	0.427	0.298	0.454
$K_{S,RM}$ (g/L)			1×10^{-12}		
$YF_{P/RM}$ (g/g)	0.160	0.293	0.265	0.227	0.175
c			1.60 ± 0.002		
$YF_{X/Xyl}$ (g/g)	0.074	0.071	0.063	0.058	0.050
$\gamma_{P,Xyl}$ (g/(g·h))	0.514	0.504	0.550	0.405	0.349
$K_{S,Xyl}$ (g/L)			$5.38 \times 10^{-2} \pm 1 \times 10^{-5}$		
$YF_{P/Xyl}$ (g/g)	0.375	0.486	0.387	0.265	0.269
d			0.100 ± 0.001		

3. Experimental Section

3.1. Sugar Maple Wood Extract Hydrolyzate and E. Coli FBWHR Strain

The details of preparation for sugar maple wood extract hydrolyzate, microorganism and cell growth, strain adaptation, fermentation, and analytical methods have been reported in [20]. Sugar maple wood chips were extracted by hot water with a wood to liquor ratio of 1:4 at about 160 °C for 2 h. Acid hydrolysis, centrifugation, and neutralization were followed to achieve the final hydrolyzate. *E. coli* FBWHR strain, successfully adapted from *E. coli* FBHW, was used in the fermentation. Batch culture experiments were carried out in a 1.3 L Bioflo 110 New Brunswick Bioreactor (New Brunswick Scientific Co., New Brunswick, NJ, USA) with a working volume of 800 mL under micro-aerobic condition. Different sugar concentrations of fermentation media were achieved by diluting concentrated hydrolyzate to 20% (v/v), 30% (v/v), 40% (v/v), 50% (v/v), and 60% (v/v) containing 30.39 g/L, 47.66g/L, 70.30 g/L, 83.75g/L and 95.33 g/L total sugar, respectively. The bioreactor was inoculated with 40 mL of actively growing 12–14 h-old culture and incubated at 35 °C. Samples (2 mL) were withdrawn intermittently and clarified by centrifugation. Supernatants were stored at −20 °C in Eppendorf Tubes (Eppendorf Inc., Westbury, NY, USA) prior to analysis.

3.2. Analytical Methods

Cell density (g/L) was estimated by using a predetermined correlation between dry weight cell concentrations (oven dry at 105 °C) *versus* optical density. Ethanol concentration was measured by gas chromatography (GC) using a Focus GC system (Thermo Scientific Inc., Austin, TX, USA) equipped with a Triplus automatic sampler and a TRACE TR-WaxMS (30 m × 0.25 mm × 0.25 μm) GC column. Sugar concentrations were determined by nuclear magnetic resonance spectroscopy (AVANCE 600 MHz NMR, Bruker, Billerica, MA, USA) using a modified two dimensional heteronuclear single quantum coherence (HSQC) experiment.

3.3. Development of Batch Fermentation Kinetic Model

The batch fermentation kinetic data of biomass growth, sugar consumption and ethanol production were used for developing the mathematical model. Model parameters were identified by minimizing the difference between experimental observations and model simulation by using ODEXLIMS, which can solve a set of ordinary differential equations by developing a general-purpose visual basic routine in Excel file [34].

4. Conclusions

Kinetic performance of ethanol fermentation in different concentrations of hot-water sugar maple wood extract hydrolyzate was investigated in batch experiments by using a recombinant strain of *E. coli* FBWHR. Higher concentration of total sugar favors the biomass growth. The highest ethanol concentration of 24.05 g/L was achieved by using an initial total sugar concentration of 70.30 g/L. The kinetic results proved that *E. coli* FBWHR is one of the most potential relevant strains for industrial ethanol production to ferment both hexoses and pentoses from concentrated hot-water wood

extract hydrolyzate. The kinetic results of cell growth, sugar utilization and ethanol production were successfully described by an unstructured model with high values of R^2 (>0.98). The findings of this study could provide insights into the process performance, optimize the process and aid in the design of processes for large scale production of ethanol fermentation from woody biomass.

Acknowledgments

Author Contributions

Yang Wang prepared the manuscript and undertook the majority of experiments as well as the data analysis presented in the paper. Shijie Liu was the supervisor of this work.

Conflicts of Interest

The authors declare no conflict of interest.

References

1. Amidon, T.E.; Wood, C.D.; Shupe, A.M.; Wang, Y.; Graves, M.; Liu, S.J. Biorefinery: Conversion of woody biomass to chemicals, energy and materials. *J. Biobased Mater. Bioenergy* **2008**, *2*, 100–120.
2. Lokhorst, A.; Wildenborg, I. Introduction to CO_2 geological storage: Classification of storage options. *Oil Gas Sci. Technol.* **2005**, *60*, 513–515.
3. Wang, Y.; Liu, S.J. Butadiene production from ethanol. *J. Bioprocess Eng. Biorefinery* **2012**, *1*, 33–43.
4. RFA: Renewable Fuels Association. Statistics, 2013. Available online: http://www.ethanolrfa.org/pages/statistics (accessed on 3 September 2013).
5. Qureshi, N.; Dien, B.S.; Liu, S.; Saha, B.C.; Hector, R.; Cotta, M.A.; Hughes, S. Genetically engineered *Escherichia coli* FBR5: Part I. Comparison of high cell density bioreactors for enhanced ethanol production from xylose. *Biotechnol. Prog.* **2012**, *28*, 1167–1178.
6. Chen, H.; Liu, S. Conversion of distillers grain to chemicals, liquid fuel and materials. *J. Bioprocess Eng. Biorefinery* **2013**, *2*, 85–93.
7. Liu, S.J.; Lu, H.F.; Hu, R.F.; Shupe, A.; Lin, L.; Liang, B. A sustainable woody biomass biorefinery. *J. Biotech. Adv.* **2012**, *30*, 785–810.
8. Field, C.B.; Behrenfeld, M.J.; Randerson, J.T.; Falkowski, P. Primary production of the biosphere: Integrating terrestrial and oceanic components. *Science* **1998**, *281*, 237–240.
9. Wang, Y.; Liu, S.J. Pretreatment technologies for biological and chemical conversion of woody biomass. *TAPPI J.* **2012**, *11*, 9–16.
10. Gírio, F.M.; Fonseca, C.; Carvalheiro, F.; Duarte, L.C.; Marques, S.; Bogel-Łukasik, R. Hemicelluloses for fuel ethanol: A review. *Bioresour. Technol.* **2010**, *101*, 4775–4800.

11. Lefebvre, B.G.; Savelski, M.J.; Hecht, G.B. Ethanol Resistant and Furfural Resistant Strains of *E. coli* FBR5 for Production of Ethanol from Cellulosic Biomass. WO2008/048513, 24 April 2008.

12. Dien, B.S.; Nichols, N.N.; O'Bryan, P.J.; Bothast, R.J. Development of new ethanologenic *Escherichia coli* strains for fermentation of lignocellulosic biomass. *Appl. Biochem. Biotechnol.* **2000**, *84*, 181–196.

13. Qureshi, N.; Dien, B.S.; Nichols, N.N.; Saha, B.C.; Cotta, M.A. Genetically engineered *Escherichia coli* for ethanol production from xylose: Substrate and product inhibition and kinetic parameters. *Food Bioprod. Process* **2006**, *84*, 114–122.

14. Ingram, L.O.; Conway, T.; Clark, D.P.; Sewell, G.W.; Preston, J.F. Genetic engineering of ethanol production in *Escherichia coli*. *Appl. Environ. Microbiol.* **1987**, *53*, 2420–2425.

15. Alterthum, F.; Ingram, L.O. Efficient ethanol production from glucose, lactose, and xylose by recombinant *Escherichia coli*. *Appl. Environ. Microbiol.* **1989**, *55*, 1943–1948.

16. Martin, G.J.; Knepper, A.; Zhou, B.; Pamment, N.B. Performance and stability of ethanologenic *Escherichia coli* strain FBR5 during continuous culture on xylose and glucose. *J. Ind. Microbiol. Biotechnol.* **2006**, *33*, 834–844.

17. Saha, B.C.; Iten, L.B.; Cotta, M.A.; Wu, Y.V. Dilute acid pretreatment, enzymatic saccharification, and fermentation of wheat straw to ethanol. *Proc. Biochem.* **2005**, *40*, 3693–3700.

18. Saha, B.C.; Iten, L.B.; Cotta, M.A.; Wu, Y.V. Dilute acid pretreatment, enzymatic saccharification, and fermentation of rice hulls to ethanol. *Biotechnol. Prog.* **2005**, *21*, 816–822.

19. Liu, T.J.; Lin, L.; Sun, Z.J.; Hu, R.F.; Liu, S.J. Bioethanol fermentation by robust recombinant *E. coli* FBHW using hot-water wood extract hydrolyzate as substrate. *Biotech. Adv.* **2010**, *28*, 602–608.

20. Wang, Y.; Liu, Z.; Chatsko, M.A.R.; Liu, S. Ethanol fermentation by *Escherichia Coli* FBWHR using hot-water sugar maple wood extract hydrolyzate as substrate: A batch fermentation and kinetic study. *J. Bioprocess Eng. Biorefinery* **2013**, *2*, 20–26.

21. Sinclair, C.G.; Kristiansen, B. *Fermentation Kinetics and Modeling*; Taylor & Francis: New York, NY, USA, 1987.

22. Marín, M.R. Alcoholic fermentation modeling: Current state and perspectives. *Am. J. Enol. Vitic.* **1999**, *50*, 166–178.

23. Lei, F.; Rotbøll, M.; Jørgensen, S.B. A biochemically structured model for *Saccharomyces cerrevisiae*. *J. Biotechnol.* **2001**, *88*, 205–221.

24. Liu, J.-Z.; Weng, L.-P.; Zhang, Q.-L.; Xu, H.; Ji, L.-N. A mathematical model for glucinic acid fermentation by *Aspergillus niger*. *Biochem. Eng. J.* **2002**, *14*, 137–141.

25. Benkortbi, O.; Hanini, S.; Bentahar, F. Batch kinetics and modelling of Pleuromutilin production by *Pleurotus mutilis*. *Biochem. Eng. J.* **2007**, *36*, 14–18.

26. Song, H.; Jang, S.H.; Park, J.M.; Lee, S.Y. Modeling of batch fermentation kinetics for succinic acid production by *Mannheimia succiniciproducens*. *Biochem. Eng. J.* **2008**, *40*, 107–115.

27. Luong, J.; Mulchandani, A.; LeDuy, A. Kinetics of biopolymer synthesis: A revisit. *Enzym. Microb. Technol.* **1988**, *10*, 326–332.

28. Garcia-Ochoa, F.; Garcia-Leon, M.; Romero, A. Kinetics modeling of xanthan production from sucrose. *J. Chem. Biochem. Eng.* **1990**, *35*, 15–20.

29. Saha, B.C.; Cotta, M.A. Continuous ethanol production from wheat straw hydrolysate by recombinant ethanologenic *Escherichia coli* strain FBR5. *Appl. Microbiol. Biotechnol.* **2011**, *90*, 477–487.

30. Swinnen, I.A.M.; Bernaerts, K.; Dens, E.J.J.; Geeraerd, A.H.; van Impe, J.F. Predictive modelling of the microbial lag phase: A review. *Int. J. Food Microbiol.* **2004**, *94*, 137–159.

31. Mercier, P.; Yerushalmi, L.; Rouleau, D.; Dochain, D. Kinetics of lactic acid fermentation on glucose and corn by *Lactobacillus amylophilus*. *J. Chem. Technol. Biotechnol.* **1992**, *55*, 111–121.

32. Choonia, H.S.; Lele, S.S. Kinetic modeling and implementation of superior process strategies for β-galactosidase production during submerged fermentation in a stirred tank bioreactor. *Biochem. Eng. J.* **2013**, *77*, 49–57.

33. Parente, E.; Hill, C. A comparison of factors affecting the production of two bacteriocins from lactic acid bacteria. *J. Appl. Bacteriol.* **1992**, *73*, 290–298.

34. Liu, S. *Bioprocess Engineering: Kinetics, Biosystems, Sustainability, and Reactor Design*; Elsevier: Oxford, UK, 2013.